# Microfluidic multiscale model of transport phenomena for Engineering and interdisciplinary education Applied to elements of a Stirling engine

Michael Krol [*1]

* Tel. ++491715775570; Email: michael_krol48@yahoo.com
1: Chemical Engineering Institute, c/o M. Kraume
Berlin University of Technology, Germany

**Abstract** Microfluidic model based on elementary mathematical tools and basic corpuscular physics is applied to flow configurations simulating the Stirling engine**.** Universality and mathematical simplicity of the model is main objective of its development. This to facilitate its application not only in micro and standard macro, single- and multiphase flows in engineering but in biology, medicine and interdisciplinary sciences as well. As dynamics of disperse systems it promotes the common physical background of multiple, apparently unrelated phenomena. Main feature of the method - compared with standard methods - is departure from differential notation where possible to ensure suitability for analysis of discontinuous systems. Physical quantities are determined directly at required scale by choice of reference volumes/surfaces and use of the mean value theorem (MVT) of integral calculus where required. Thus the method is applicable to discrete particles and avoids higher order requirements of Navier-Stokes solutions. Besides saving one integration step it generally facilitates the analysis considerably. Newton's second law is used explicitly as single equation of motion. Together with conservation laws it is applied to non-relativistic motion of particle systems in range from individual particles, atoms, molecules or even electrons, over to macroscopic particle sets in solid or flowing systems of traditional mechanics, up to celestial bodies of classical astro-physics. The basically microfluidic model was used to derive all definitions and equations of standard continuum fluid mechanics and multiphase flows. Compared with standard methods the here used model has the singular ability to describe consistently all phenomena related to one of most inspiring technical devices: to Stirling engine.

**Keywords:** single- and multiphase flows, turbines, engines, thermodynamics, interdisciplinary education

**1. Introduction** Purpose of this work is simplest possible mathematical model dealing with transport processes at all technically relevant scales [13- 21] with help of a minimum of basic concepts of corpuscular physics [2,3,8,9]. The model is designed to facilitate interdisciplinary education. It may be used to describe all transport phenomena (energy or matter) in systems built of particles respectively discrete elements (eg. cells of biological systems, machine parts etc.) characterized by mass and velocity (momentum)**.** Engineering applications start with motion of elementary particles [2,3,8,9], heat flow and generation, classical single and multiphase flows over to non-relativistic astrophysics [6, 14 - 21]. Difference between the proposed method and classical methods of fluid mechanics [1, 5][4] is applicability of a single, very limited set of basic concepts and equations to the possibly broadest range of phenomena.

Stirling engine using external temperature differences serves as example of a technical device touching a broad range of transport phenomena. Discussion will be limited to three versions of this engine: classical piston engine ("heated air" resp. engine with external combustion chamber [e.g. 11]), flow in fixed circular and in rotating circular systems with zero total momentum change. Two latter versions represent alternative realizations of the Stirling cycle. Relevant for these configurations is heat transfer, definitions of temperature, pressure, viscosity of fluid media, changes of aggregate state like boiling, evaporation, condensation etc.. It will be shown that all these phenomena may be coherently discussed in terms of Newton's second law as single equation of motion and conservation laws.

## 2. Numerical Model – method

Generally valid physical considerations [18, 21] independent of construction features are - because of their general relevance - below briefly repeated in summarized form:

Newton‘s equation of motion applied to an arbitrary material disperse system defines its physical properties and the involved forces in terms of momentum exchange starting at atomic level [2,3, 15-21](Fig. 1 below):

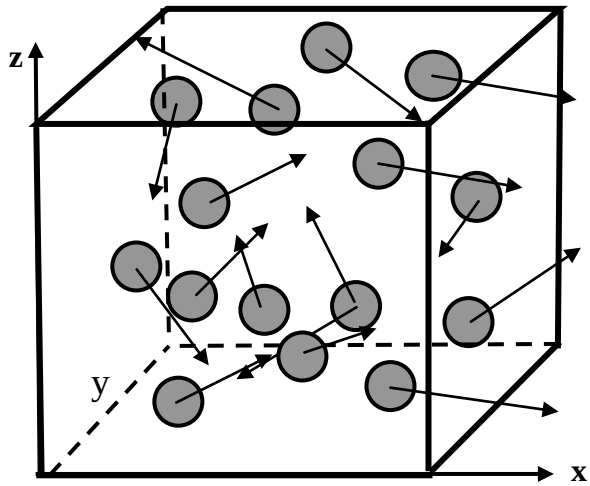


**Fig. 1**: Fluid modelled as a molecular/atomic disperse system [2,3, 15 - 21]. Schematically shown are gas molecules in stochastic thermal motion. Arrows symbolize the thermal molecule velocities.

Newton’s law used here to define interaction forces in particle systems (molecules, cells, machine parts) reads [18-21]:

$$\underline{F} = \frac{d}{dt}\int_V \rho\,\underline{v}\,dV \qquad (1)$$

The right side of the above equation represents the total time rate of change of momentum in volume V (i.e. mass times acceleration = m $\underline{a}$ in case of rigid/solid bodies) with density ρ(dV) within time interval dt. Vectors are marked by underlining.

Time rate of momentum change expressed in terms of momentum conservation [1,15-21] as sum of local momentum changes and momentum fluxes through boundaries A of the control volume V reads:

$$\underline{F} = \frac{d}{dt}\int_V \rho\,\underline{v}\,dV = \frac{\partial}{\partial t}\int_V \rho\,\underline{v}\,dV + \int_A \rho\,\underline{v}\,\underline{v}\bullet\underline{dA} \qquad (2)$$

$\underline{dA}$ are oriented, vector elements of surface A. Similarly mass conservation law [1,15-21]:

$$\frac{d}{dt}\int_V \rho\,dV = \frac{\partial}{\partial t}\int_V \rho\,dV + \int_A \rho\,\underline{v}\bullet\underline{dA} \qquad (3)$$

Heat transfer in a particle system is explained in terms of stochastic, thermal molecule momentum [15-21]. Thereby useful is the non-vanishing quadratic mean value of the thermal molecule velocity $\underline{v}_\lambda$ along the mean free molecule travelling path λ in volume V. Using the general structure of conservation laws [1] we write [15 - 21]:

$$\frac{d}{dt}\int_V \rho\,v_\lambda^2\,dV = \frac{\partial}{\partial t}\int_V \rho\,v_\lambda^2\,dV + \int_A \left(\rho\,v_\lambda^2\right)\underline{v}\bullet\underline{dA} \qquad (4)$$

Statistical physical fluid properties respectively “bulk fluid quantities” like pressures p, fluid densities ρ and viscosities η follow in terms of averaged particle-particle interactions at micro scale [2, 15-21]. Thereby, equations (1–4) are applied to microscopic molecular motions through suitably defined control surface e.g. A (x-0-y), perpendicular to z-axis and containing the x and y –axis Fig. **2** below.

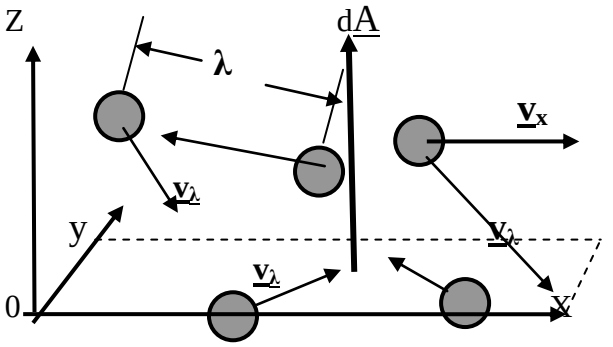


**Fig. 2:** Molecule transport through control surface: x-0-y. λ is symbolic representation of (averaged) collision free path. $\underline{V}_\lambda$ is vector of thermal velocity of a molecule. $\underline{V}x$ symbolizes vector of superimposed average bulk flow

Thermal gas pressure: from eq. (2) in reference to Figs. 1, 2 and assumption:

$v_\lambda(z \pm \lambda) = v_\lambda(z)$ it follows [15- 21]:

$$p = \rho_G\, v_{\lambda Z}^2 \qquad (6)$$

Together with molecular binding forces [2, 21] thermal pressure defines the melting point of

solids and the boiling point of liquids [2]. Result (6) shows in particular, that:
Temperature T is an indicator of the average stochastic molecular velocities [15-21]:

$$T = k\, v_{\lambda Z}^2 \qquad (7)$$

Gas laws: density $\rho_G(V)$ in (6) expressed by molecule numbers and masses, with R the universal gas constant [1, 2] R≈8.314 J/mol K it follows [18 - 21]:

$$\frac{p\,V}{T} = n_m\, R = const \qquad (8)$$

Heat conductivity: with:

$$v_\lambda^2(x \pm \lambda) = v_\lambda^2(x) \pm \lambda \frac{\partial\, v_\lambda^2}{\partial x} \qquad (9)$$

inserted in eq. (4) it follows [18-21]:

$$\left.\frac{\partial\, \Theta_C}{\partial t}\right|_{V_R} = \frac{\partial}{\partial t} \int_{V_R} \rho_G\, v_\lambda^2\, dV =$$

$$= -\rho_G\, v_{(\lambda x)}\, \lambda \frac{\partial\, v_\lambda^2}{\partial x} A_X \qquad (10)$$

Thereby $\Theta_C$ is the content of heat momentum in the considered volume $V_R$ of a substance. Product: $\rho_G\, v_{(\lambda x)}\, \lambda$ defines the coefficient of thermal conductivity κ [18, 21]:

$$\kappa = \rho_G\, v_{(\lambda x)}\, \lambda \qquad (11)$$

Fourier's law of heat conductivity [18- 21]:

$$\frac{\partial\, \Theta_C}{\partial t} = -\kappa\, A_X \frac{\partial T}{\partial x} \qquad (12)$$

Change of thermal momentum Θ follows as [18,21]: $\Delta\Theta = C_S\, m\, \Delta T$ with heat capacity $C_S$, mass $m = \rho\, V$ and volume $V = \delta\, A_X$ when δ = thickness of considered volume V. Thus:

$$\frac{\partial\, T}{\partial t} = -\frac{\kappa}{C_S\, \rho\, \delta} \frac{\partial T}{\partial x} \qquad (13)$$

Dynamic viscosity follows [2, 15- 21] from eq. (2) under assumption (Fig. 2 above) that:

$$v_x(z \pm \lambda) = v_x(z) \pm \lambda \frac{\partial v_x}{\partial z} \qquad (15)$$

Eq. (2) with inserted assumption (15) defines the statistical average of the friction force as:

$$F_{T,X} = \rho_G\, v_{\lambda z}\, \lambda\, A_z \frac{\partial v_x}{\partial z} \qquad (16)$$

Dynamic viscosity results accordingly as [2,15-21]: $\eta = \rho_G\, v_{\lambda z}\, \lambda$ (17)

Forces in macroscopic flows: in terms of averaged molecular interactions and "bulk fluid properties" (above) it follows [13-21]:

$$\frac{d}{dt} \int_V \rho \underline{v}\, dV = \int_V \rho \underline{g}\, dV - \int_A p \underline{dA} + \int_A \underline{\underline{t}} \bullet \underline{dA} \qquad (18)$$

Forces on the right side of (18) are sequentially identified as [13 - 21]: gravity **g**, pressure p, friction $\underline{\underline{t}}$ etc. acting in volume V and on its limiting surfaces A. Double underlining denotes the considered term (here $\underline{\underline{t}}$) as a matrix/ (respectively: tensor of second order).

## 3. Results and Discussion

**3.1** Piston versions of Stirling engine

Relevance of definitions (1-18) for classical Stirling engines implies (Fig. 3 below):

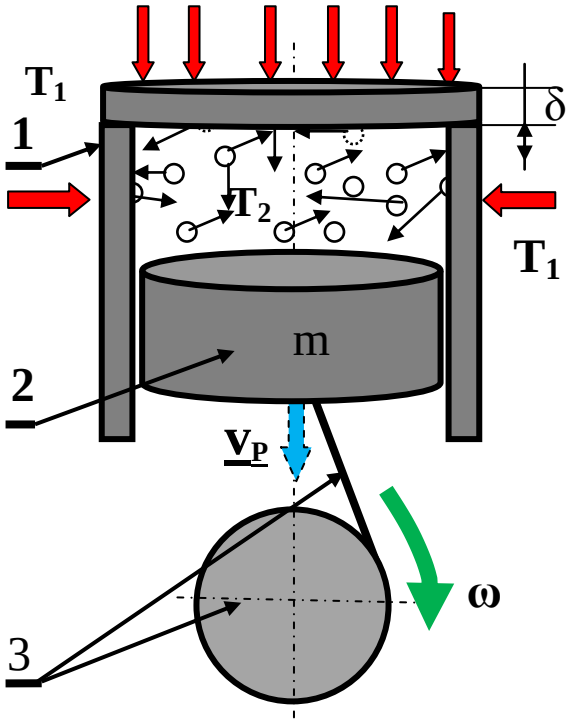


**Fig. 3:** Piston version of a Stirling engine.
**1** - piston chamber with wall thickness **δ**
**2** - rigid piston of mass **m**
**3** - crankshaft – generator connection
$\mathbf{T_1}$ – Temperature outside piston chamber
$\mathbf{T_2}$ - Temperature inside piston chamber
In above shown operation step is $\mathbf{T_1 > T_2}$. Red arrows imply direction of heat transport, which in piston version changes periodically. In next step situation must reverse to $\mathbf{T_1 < T_2}$.

**$T_1 > T_2$ :** Heat transport from outside of piston

chamber into gas filled space over the piston in Fig.3. Gas temperature above the piston increases. Increasing gas temperature causes gas expansion and pushes the piston downwards with velocity $\underline{\mathbf{v}}_p$. Crankshaft and generator are being turned in graphically implied direction **ω**.

$T_1 < T_2$ **:** Heat transport from gas filled space over the piston to outside space. Gas temperature above the piston decreases. Decreasing gas temperature causes reduction of gas volume over the piston and pushes it upwards (piston velocity $\underline{\mathbf{v}}_p$ is reversed)

Disadvantage of the piston version of a Stirling engine is discontinuous heat transport in and outside of piston chamber. Additional designing effort and energy losses proportional to thickness δ of the piston chamber are consequence. Circular realizations of thermodynamically slightly modified Stirling cycle aim at reduction of these disadvantages.

**3.2** Fixed circular realization of Stirling cycle (Fig. 4 below).

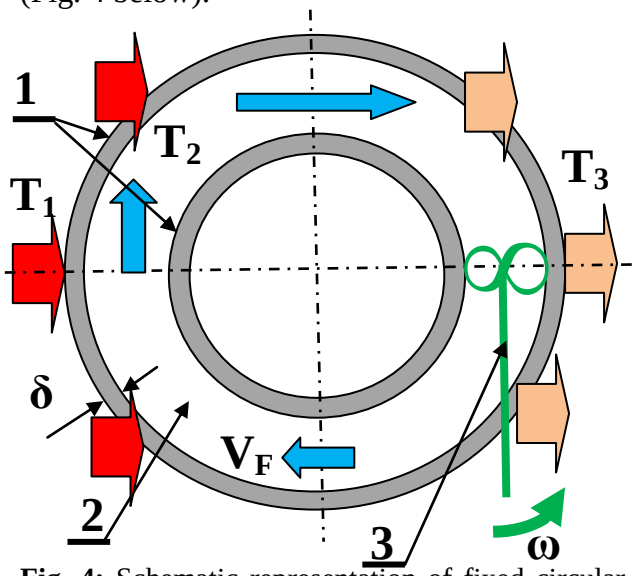


**Fig. 4:** Schematic representation of fixed circular version of modified Stirling cycle.
**1** - walls of circular ring with wall thickness **δ**
**2** - fluid filled fixed ring with fluid density **ρ**
**3** - turbine – generator connection
$\mathbf{T_1}$ - Temperature on the left side of fluid chamber
$\mathbf{T_2}$ - Temperature inside fluid chamber
$\mathbf{T_3}$– Temperature on the right side of fluid chamber
Here is constantly $\mathbf{T_1 > T_2 > T_3}$ so that red arrows imply irreversible direction of heat transport.

Stirling engine shown in Fig. 4 imitates roughly the global water transport on earth. It consists of a rigid torus filled with liquid (or gas). Liquid in configuration shown in Fig. 4 is being permanently heated on its left side (equator in relation to global water transport on earth), so that $T_1 > T_2$ and cooled in the right part. (In respect to global water transport water vapour clouds rising above equator correspond with heated fluid leaving left torus part. Rivers in the northern hemisphere correspond to fluid vapour condensed in the cooled right torus part: circular flow shown in Fig. 4 implies that all water power plants and rivers on earth are elements of a giant Stirling engine powered by the sun).

Its main operation properties (Fig. 4) are:

- Density of heated fluid in the left torus half $\boldsymbol{\rho_{LH}}$ decreases in consequence of rising thermal velocities of fluid molecules respectively temperature [18- 21] (Fig. 5, below)

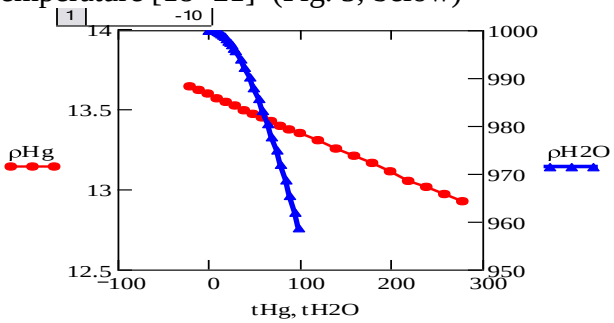


**Fig.5** Densities of mercury (red line) and water (blue line) [7] plotted over temperature in °C.

- Viscosity of heated liquids in the left torus half $\boldsymbol{\eta_{LH}}$ decreases with rising temperature. [7, 18- 21], (Fig. 6, below):

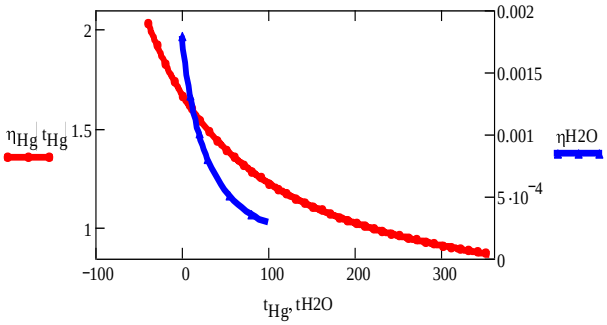


**Fig. 6** Viscosities of mercury (red line) and water (blue line) [7] plotted over temperature in °C.

- Difference of hydrostatic pressures $\Delta p_{RL}$ [18-21] caused by falling fluid density in the heated left part of torus $\boldsymbol{\rho_{LH}}$ initiates fluid flow

implied in Fig. 4 by blue arrows.

$$\Delta p_{RL} = g\,D\,(\rho_{RH} - \rho_{LH}) \qquad (19)$$

Thereby g is gravitational acceleration, D diameter of the torus and $\rho_{RH}$ and $\rho_{LH}$ are fluid densities in the right and left torus half.

- Maximum of fluid flow velocity caused by the driving temperature difference $\Delta T=T_1-T_3$ occurs at temperatures $T_2$ of the fluid close to its boiling point. This not only because density of the liquid itself reaches a minimum but because of vapour bubbles forming in the liquid and allowing the density $\rho_{LV}$ of thus created liquid-vapour multiphase flow (index: $_{LV}$) to assume values between density of liquid at boiling temperature $\rho_{LTmax}$ and density of vapour at given pressure and boiling temperature $\rho_{VTmax}$:

$$\rho_{VTmax} \leq \rho_{LV} \leq \rho_{LTmax} \qquad (20)$$

Flow velocity maximum in a fixed circular Stirling cycle is shown in Fig. 7 below.

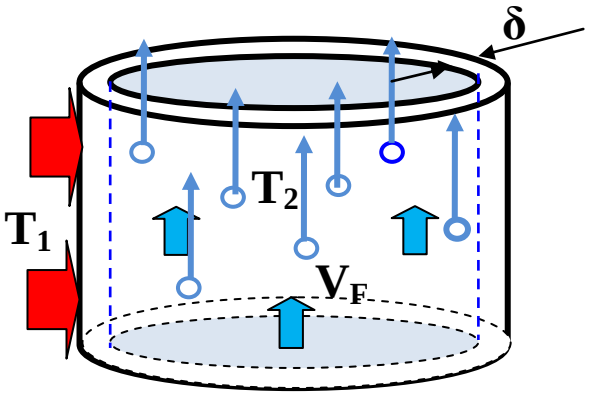


**Fig. 7:** Segment of a fixed circular version of modified Stirling cycle indicating flow of boiling liquid $V_F$ with rising spherical vapour bubbles. Relative vapour content [18-21] is ε: ε = 0 for vapour free flow. ε = 1 for fully vaporized flow.
**$T_1$** - Temperature on the left side of fluid chamber
**$T_2$** - Temperature inside fluid chamber

Behaviour of liquid-vapour flow shown in Fig. 7 may adequately be described by eq. 18:

$$\frac{d}{dt}\int_V \rho\,\underline{v}\,dV = \int_V \rho\,\underline{g}\,dV - \int_A p\,\underline{dA} + \int_A \underline{\underline{t}}\,(\eta,\zeta)\bullet\underline{dA}$$

Flow in fixed torus shown in Figs. 4,(7) may exhibit two basic flow modes at constant boiling temperature. Depending on amount of delivered heat energy, possible is:

**a.** Vapour free flow of liquid provided with just enough heat to keep temperature at boiling level but free of vapour bubbles. Relative bubble content ε is: ε = 0. Flow velocity is determined by difference of hydrostatic pressures ([20] rel. 19 above) between cooled (index: $_C$) and heated (index: $_H$) halves of torus shown in **Fig 4** i.e. by [20]:

$$\Delta p_{RL} = g\,D\,(\rho_C - \rho_H) \qquad (21)$$

**b.** Fully vaporized flow – enough heat is delivered to vaporize whole liquid. Relative bubble content ε = 1.

Interpolation between conditions 1 and 2 (above) for vapour content ε in range: $0 \leq \varepsilon \leq 1$ results in the driving pressure difference**:**:

$$\Delta p_{1\text{-}2} \approx \left[\rho_{LC} - (1-\varepsilon)\rho_{LH}\right] g\,D - \varepsilon\rho_V\,g\,D \qquad (22)$$

Indices: $_L$ : liquid phase, $_G$ or $_V$ : gas or vapour, $_C$ : cold, $_H$ : heated. Approximation of resulting velocity $v_x$ of vapour bubble free flow in fixed torus is shown in **Fig.8** below.

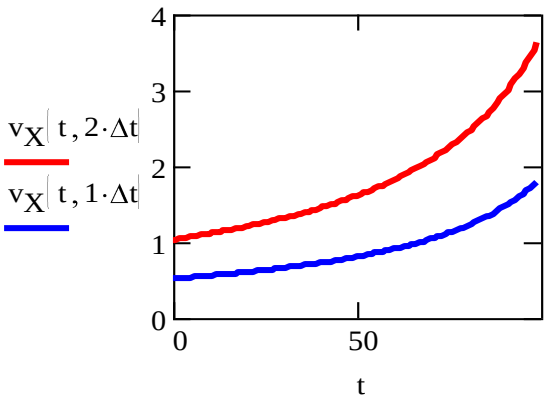


**Fig.8** Flow velocity of bubble free water flow for different temperature differences between heated and cooled halves of fixed torus shown in **Fig. 4** above. Flow velocity increases with higher temperatures in heated torus half. Upper red line: flow velocities for temperature difference Δt≈ 2°C. Blue line:: temperature difference Δt≈ 1°C.

Vapour bubbles, developing with increasing heat delivery, have manifold influence on flow velocity. First they increase flow velocity by diminishing the overall density of liquid-vapour mixture (above). Further bubbles rising in flowing liquid exert additional "friction" accelerating liquid in their vicinity and thus increasing slightly the overall flow velocity. This effect is shown in **Fig. 9** below.

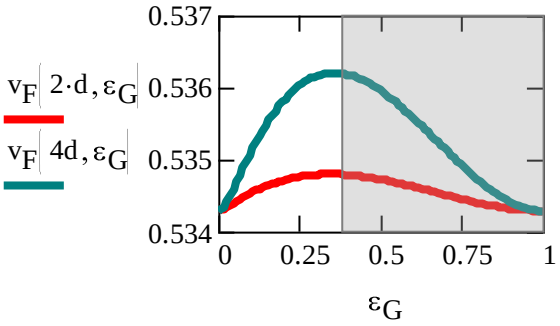


**Fig. 9** Vapour bubbles increase upward flow velocity of liquid in heated part of torus (Figs. 4/7. Flow velocity increases with growing bubble size: 2d= 2 mm (lower red line) and 4d= 4 mm (higher blue line). Maximum of flow velocity at ε > ca. 0.33 marks begin of transition to fully vaporized flow (grey marked field).

Decrease of liquid flow velocity at void fraction ε > 0.33 (Fig. 9), marks begin of transition to fully vaporized flow requiring construction changes (e.g. Fig. 10 below) due to necessary pressure control.

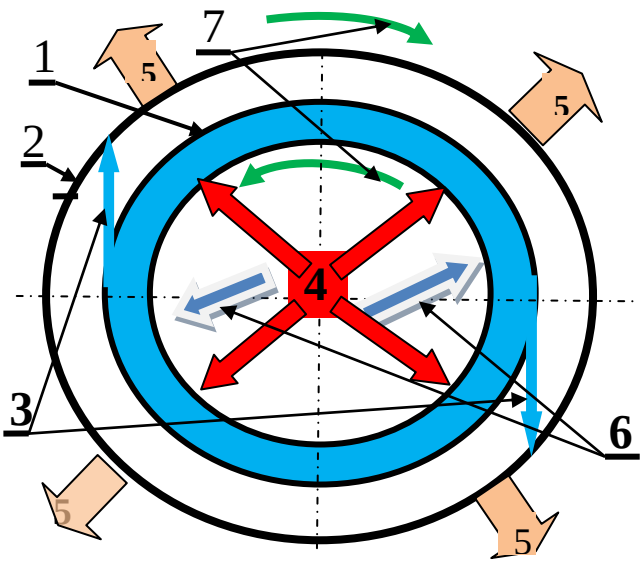


**Fig. 10** Rotating heated torus (**1**) placed in closed external condensation chamber (**2**).
**3** – Jet streams (3) of pressurized condensed vapour escape from constantly heated **(4)** rotating torus (**1**) into closed, externally cooled (**5**) condensation chamber (**2**).
**6** – Centrifugal forces press cooled vapour back into heated rotating torus (**1**) Green arrows (**7**) show opposite rotation directions of heated torus **(1)** and externally cooled (**5**) condensation chamber **(2)**.

**3.3** Rotating circular torus shown in Fig. 10 (above) offers advantages for overall efficiency. A basic characteristic of this construction is vapour driving the torus by sideward jet streams entering external condensation chamber as implied in **Fig. 10**. Vapour entering condensation chamber imparts its momentum to condensation chamber itself, so that it starts rotating in direction opposite to that of heated torus. However, in this case total momentum change is zero, as sum of mutually opposite rotation momenta of torus and of condensation chamber. Centrifugal forces are thereby used to compress vapour and to pump it back into the torus thus closing the cycle. It is self-evident that in both cases of above described circular Stirling cycle realizations all initially implied application possibilities: micro and macro of the described model [18 - 21] are relevant. Thereby micro and nano aspects are of special meaning in the latter - rotating torus – version since thermal molecule velocities determine the velocity [18,20,21] of vapour jet streams from torus into condensation chamber. Fig. 11 (below) signifies relevance of this model aspect [20] to the above discussed topic.

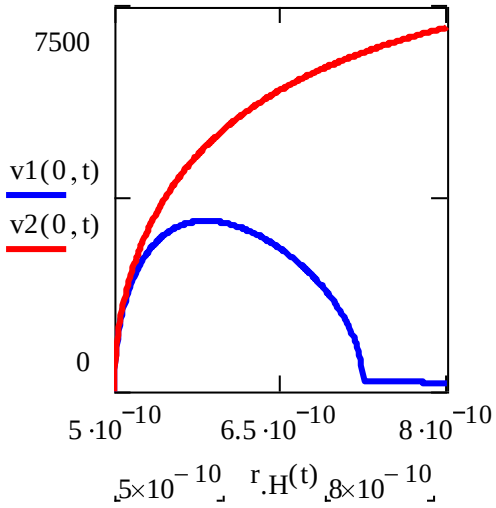


**Fig. 11** Velocities of model particles [20] outlining application boundaries of circular Stirling cycles: lower blue line implies that the fixed circular Stirling device uses rather effects limited to heating and cooling of liquid phase, upper red line implies that in the rotating heated torus almost unlimited phase changes and molecule velocities are allowed.

Fig. 11 implies that the fixed heated torus device (Figs. 4/7) is limited to flow caused mainly by hydrostatic pressure differences. Rotating heated torus (Fig. 10) is free of this limitation. Further details: [18-21].

**Conclusions:** Explicit application of Newton's second law and conservation laws in differential-integral notation [1, 13 - 21] to fluids modelled as molecular disperse systems [15 - 13], provides a self-consistent, physically coherent, concise and simple description of all non - relativistic transport phenomena. Set of equations to remember is very small and provides a transparent common physical background for applications not only in process engineering but in all disciplines in which transport processes are relevant (e.g. medicine, biology, geophysical sciences etc. respectively interdisciplinary education)

In view of experimental evidence in fields of corpuscular physics, kinetic gas theory [2, 3], as well as in classical astrophysics [6], Newton's law represents experimentally best confirmed physical law describing non-relativistic motion of matter. It provides adequate reference basis and starting point of motion analysis in all material systems.

**Acknowledgments:** author is particularly grateful to prof. F. Ebert of University Kaiserslautern for the initial challenging impulse [12] and prof. M. Kraume and Technical University of Berlin for moral support and patience.

**Nomenclature:**

| | | |
|---|---|---|
| A | [$m^2$] | Surface, area |
| $C_S$ | [J/K kg] | Heat capasity |
| D | [m] | Diameter |
| F | [N] | Force |
| G | | Index: gas |
| g | [$m^2$/s] | Gravitational acceleration e.g. in earth's gravitational field |
| k | | Experimental constant, units as required by equation |
| m | [kg] | Mass |
| p | [$N/m^2$] | Pressure |
| R | [m] | Radius, otherwise: |
| R | [J/mol K ] | Universal gas constant [1, 2] R≈8.314 J/mol K |
| S | | Index: specific |
| t | [s] | Time |
| T | [K] | Temperature |
| v | [m/s] | Velocity |
| V | [$m^3$] | Volume |
| x,y,z | | Axis directions of Carthesian coordinate system, Index: component along a given coordinate axis |
| δ | [m] | Thickness |
| Δ | [-] | Increment e.g. ΔT: temperature change |
| ε | [-] | Relative bubble content |
| λ | [m] | Average free molecule path |
| ρ | [$kg/m^3$] | Density |
| η | [Pa s] | Dynamic fluid viscosity |
| κ | [W/K m] | Heat conduction coefficient |
| $\Theta_C$ | [kg $m^2/s^{3]}$] | Content of heat momentum in a volume |
| Ω | [1/s] | Angular rotation velocity |

All other here not mentioned symbols and indices are described in text

**References**

[1] Hughes, W.F.; Brighton, J.A.; Fluid Dynamics; Schaum´s Outline Series in Engineering; McGraw-Hill Book Co.; 1967

[2] Reif, F.; Statistical Physics; McGraw-Hill Book Company; 1967

[3] Resnick, R; Halliday, D.; Physics; J. Wiley and Sons, Inc.; 1966

[4] Fefferman; Ch.; L.; Existence and smoothness of the Navier-Stokes equation; Princeton; NJ 08544-1000; 2000

[5] Hirsh, C.; Numerical Computation of Internal and External Flows; Elsevier; 2007

[6] Hoyle; F; Astronomy and Cosmology; Freeman and Co.; 1975

[7] Grigull, U.; Blanke, W.; Stoffwerte; Springer Vlg.; 1989.

[8] Wichmann; H.,Eyvind; Quantum Physics; Berkeley Physics Course – Volume 4; McGraw – Hill Book Company; 1971

[9] Purcell; M. Edward; Electricity and Magnetism; Berkeley Physics Course – Volume 2; McGraw – Hill Book Co.; 1965

[10] Marsden,J.E.; Tromba, A.J.; Vector Calculus; Freeman and Co.; 1976

[11] Encyclopaedia Britannica, 1976

[12] Krol, M.; Experimentelle Untersuchung der Partikelbewegung bei hohen Feststoff-Konzentrationen in turbulenten Mehrphasen-Strömungen; Phd. Thesis; University of Kaiserslautern; 1984

[13] Krol, M.; Prediction of relative particle fluid displacements in flowing suspensions at medium particle volume fractions by means of a simple stochastic model; 4th Miami Int. Conf. on: Multiphase Transport and Particulate Phenomena; Miami, USA; 1986; Multiphase Transport and Particulate Phenomena; Vol. 4; Hemisphere Publishing Corporation and Springer Publishing House (1988).

[14] Krol, M.: Pressure drop in porous media at arbitrary Reynolds numbers; European Aerosol Conference; Helsinki; Sept. 1995;

[15] Krol, M.: Fluiddynamik – Dynamik disperser Systeme; 1997/98

[16] Król, M.: Equation of Motion of a compressible Fluid derived from the Kinetic Theory of Gases and Newton's Second Law; Reports of the Polish Academy of Sciences; IMP PAN Rep. No. 3195/2003 and IMP PAN Rep. No. 3197/2003

[17] Król, M.; Physics of solids, liquids and gases; Lectures (GSW); Poland; 2005 - 2010

[18] Krol, M.; Physikalische Grundlagen der Ein- und Mehrphasen-Strömungen; Lectures at Technical University Berlin; Germany, since 2006

[19] Krol, M.: Momentum Exchange as common physical background of a transparent and physically coherent description of Transport Phenomena; Begell House Inc. Proceedings of the International Symposium "Turbulence, Heat and Mass Transfer 6";2009.

[20] Krol, M.; Significance of the microfluidic concepts for the improvement of macroscopic models of transport phenomena; paper with appendix submitted to the 3rd Micro and Nano Flows Conference, Thessaloniki, Greece; 2011. By courtesy of Brunel University, UK in internet under: michael_krol48

[21]Krol,M.; Dynamik-disperser-systeme; 2012
http://bookboon.com/de/studium/ingenieurwesen/dynamik-disperser-systeme